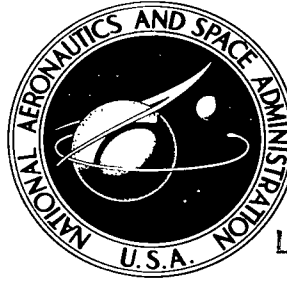


NASA TECHNICAL NOTE



NASA TN D-2592

C.1

LOAN COPY: P. 100-1000
AFWL (CCL) 2
KIRTLAND AFB, TX

NASA TN D-2592



FRAGMENTATION OF ANTHRACENE IN AN ELECTRON-BOMBARDMENT ION SOURCE

*by Nelson L. Milder
Lewis Research Center
Cleveland, Ohio*



0154695

FRAGMENTATION OF ANTHRACENE IN AN ELECTRON-
BOMBARDMENT ION SOURCE

By Nelson L. Milder

Lewis Research Center
Cleveland, Ohio

NATIONAL AERONAUTICS AND SPACE ADMINISTRATION

For sale by the Office of Technical Services, Department of Commerce,
Washington, D.C. 20230 -- Price \$1.00

FRAGMENTATION OF ANTHRACENE IN AN ELECTRON- BOMBARDMENT ION SOURCE

by Nelson L. Milder

Lewis Research Center

SUMMARY

Fragmentation of anthracene in a 5-centimeter-diameter version of a Lewis electron-bombardment ion source was studied with the aid of an electric quadrupole mass spectrometer. Seven to nine peaks of comparable intensity were observed corresponding to specific masses ranging from about 20 to 178 atomic mass units per unit charge. The variation in relative peak heights as a function of electron emission current and ion discharge voltage is presented. Emission currents ranged from 10 to 760 milliamperes and the ion discharge voltage ranged from 40 to 140 volts. The experiment demonstrated that severe fragmentation of anthracene occurs even under minimum conditions of sustained ion discharge.

INTRODUCTION

For the purpose of improving the performance and extending the applicability of the Lewis electron-bombardment thruster, it would be desirable to employ heavy particles such as molecules with a high molecular weight (ref. 1). A recent investigation (ref. 2) of high-molecular-weight materials indicated on the basis of thrust target measurements that extensive fragmentation of such heavy molecules occurs in the ionization chamber for electron emission currents ranging from about 0.5 to 2.6 amperes. From the data obtained in reference 2 it was conjectured that molecular fragmentation could be reduced by employing electron emission currents less than 0.5 ampere; however, the data in this range were inconclusive.

In the present study, which was complementary to that of reference 2, an electric quadrupole mass spectrometer (refs. 3 to 7) operated in conjunction with an electron-bombardment ion source was used to study the fragmentation of anthracene ($C_{14}H_{10}$) for electron emission currents less than 1 ampere and ion discharge voltages ranging from 40 volts to 140 volts.

Anthracene is a fused-ring aromatic hydrocarbon. There are theoretical bases for expecting this molecule to provide a stable primary structure for heavy molecule propel-

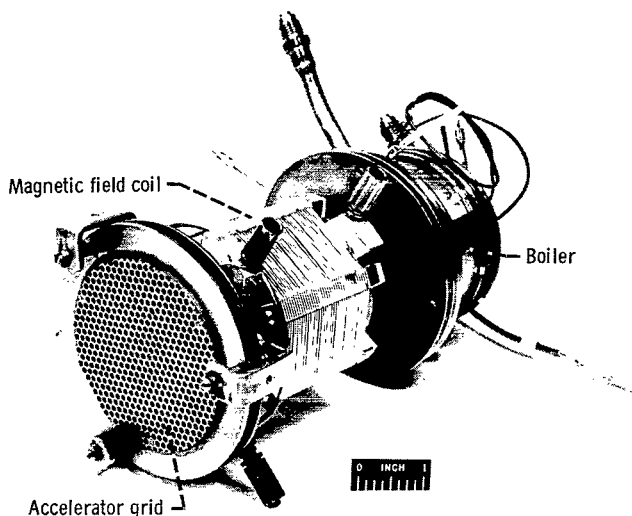


Figure 1. - Electron-bombardment ion source.

lants (ref. 8). Electron impact studies of anthracene have been reported (ref. 9) and tend to support this expectation. The thrust target measurements of reference 2, however, indicated a more severe fragmentation than reported in reference 9.

The discharge obtained in the source described herein approximates that obtained in the Lewis electron-bombardment thruster (ref. 10). Thus, the resulting mass analysis of the ion beam can be used to demonstrate the effect of source parameters on propellant ionization and fragmentation at low plasma density (electron emission currents less than 1 amp), where the experimental error of reference 2 was greatest.

Following a description of the ion source, mass spectrometer and experimental configuration, a discussion of the variation in the spectral intensities with electron emission and ion discharge voltage will be presented.

DESCRIPTION OF EXPERIMENT

Apparatus

Ion source. - The ion source used in this study (fig. 1) was a geometrically half-scaled version of the Lewis 10-centimeter (anode diameter) electron-bombardment ion thruster. The principles underlying the operation and performance of such thrusters are presented in references 11 to 13. A schematic diagram showing the ion-source configuration and its associated power supplies is presented in figure 2.

A steam-heated boiler served to vaporize the propellant material. The vapor entered the ion discharge chamber through an orifice and distributor. A tantalum wire filament (20 mils in diameter) mounted coaxially within the 5-centimeter-diameter cylindrical anode provided electron emission currents ranging from 10 to 760 milliamperes. A magnetic field coil was wound concentrically about the discharge chamber. The magnitude of the field along the source axis was approximately 30 gauss.

The ions produced by electron bombardment were extracted from the source by means of two grids spaced 0.32 centimeter apart. The net ion accelerating voltage was maintained at 300 volts. The ion discharge potential difference ranged from 40 to 140 volts.

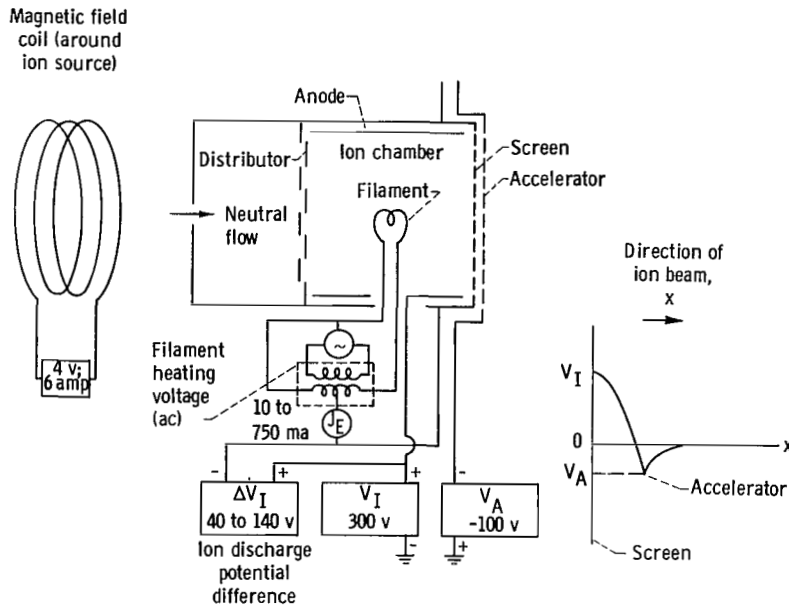


Figure 2. - Schematic diagram of electron-bombardment ion source.

Electric quadrupole mass spectrometer. - The technique of the strong-focusing electric quadrupole mass spectrometer has been well documented (refs. 3 and 4). It will suffice to present herein a rather abbreviated discussion in order to familiarize the reader with the general principles of spectrometer operation.

Physically, a beam of ions enters the analyzer portion of the spectrometer through a small entrance aperture. The analyzer consists of four electrodes arranged symmetrically about the analyzer axis. Voltages applied to these electrodes serve to establish an oscillating electric field in the region enclosed by the electrodes. Ions entering this field will be rejected or transmitted according to their charge-to-mass ratio. Transmitted ions are collected at the exit of the analyzer and are monitored as an ion current.

Figure 3 is the cross section of a symmetric hyperbolic electrode configuration, including the associated applied voltages and electrical connections. The cartesian axes x and y are in the plane of the figure, while the z -axis (axis of symmetry) is normal to

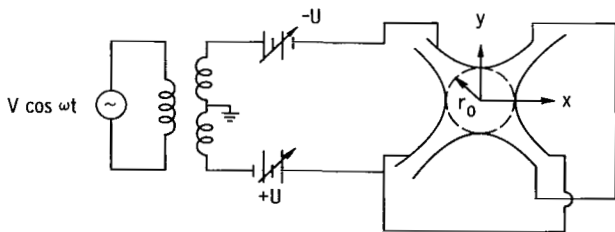


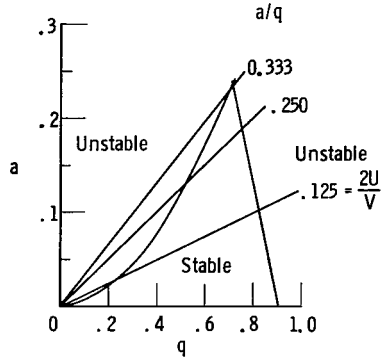
Figure 3. - Cross section of symmetric hyperbolic electrode configuration showing electrical connections.

the plane of the figure. The parameter r_0 specifies the radius of the focusing field. The voltage applied to the electrode is, from reference 3,

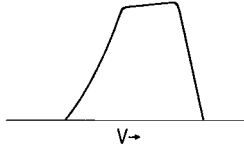
$$\Phi_0 = U + V \cos \omega t \quad (1)$$

(All symbols are defined in the appendix.)

The radio-frequency voltage is applied



(a) Stable and unstable regions.

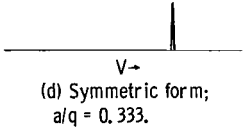


(b) Trapezoidal form;
a/q = 0.125.

Relative intensity



(c) Intermediate form;
a/q = 0.250.



(d) Symmetric form;
a/q = 0.333.

Figure 4. - Stability region and characteristic line shapes.

between the positive and negative electrodes such that the z-axis is maintained at ground potential.

The resulting field potential is

$$\Phi = (U + V \cos \omega t) \frac{x^2 - y^2}{r_0^2} \quad (2)$$

If the quantities ξ , a , and q are defined such that

$$\xi = \frac{\omega t}{2} \quad (3)$$

$$a = \frac{8eU}{mr_0^2 \omega^2} \quad (4)$$

and

$$q = \frac{4eV}{mr_0^2 \omega^2} \quad (5)$$

the equations of motion for singly charged ions can be written as

$$x'' + (a + 2q \cos 2\xi) x = 0 \quad (6)$$

$$y'' - (a + 2q \cos 2\xi) y = 0 \quad (7)$$

$$z'' = 0 \quad (8)$$

where the primes indicate differentiation with respect to ξ . The parameters a and q play a fundamental role in quadrupole operation. It should be noted from equation (8) that the focusing field has no effect on ion motion along the symmetry axis.

The solutions to equations (6) and (7) are dependent on the parameters a and q (ref. 14). The nature of this dependence is such that solutions will either be bounded (stable) or exponentially divergent (unstable) in time. The relation between these solutions and spectrometer operation can be best understood with the aid of figure 4.

Figure 4(a) shows regions in the (a, q) plane for which solutions to equations (6) and (7) (ion trajectories) are stable or unstable. The actual spectrometer operating point is determined by the ratio

$$\frac{a}{q} = \frac{2U}{V}$$

A convenient mode of operation is along lines of constant slope a/q . The intersection of such lines with the stability region boundaries determines spectral line widths.

The spectrometer used in this study employed fixed values of the applied radio frequency and field radius; therefore, as shown by equation (5), q is a linear function of the radio-frequency voltage V for a particular ion mass and charge. The general forms of the resulting spectral lines are presented as a function of the applied radio-frequency voltage in figures 4(b) to (d), varying from the trapezoidal form of 4(b) to the symmetric form of 4(d) (ref. 3). It should be noted that the maximum intensity occurs at a value of V for which $q = 0.706$.

Line shapes such as those of figure 4 serve to define spectrometer resolution. Resolution can be defined as the value of V at maximum intensity divided by the voltage difference ΔV across the width of the spectral line at half maximum intensity. This definition is proportional to the generally used definition of resolution (ref. 3),

$$\frac{m}{\Delta m} \propto \frac{V}{\Delta V} \quad (10)$$

where m is the ion mass (assuming unit charge) at the peak maximum, and Δm is the line width (in units of mass) at half maximum intensity. It is convenient to use the definition of resolution in terms of mass units when identification of complicated spectra is required. The definition in terms of the peak radio-frequency voltage is operationally useful when spectrometer scanning is accomplished by sweeping voltage.

Theoretically, the slope of the operating line determines the spectral resolution. It can be shown (ref. 3), however, that the maximum resolution attainable depends on spectrometer frequency and length, net ion accelerating voltage, and charge-to-mass ratio as follows:

$$\frac{m}{\Delta m} = \frac{4.2 \times 10^2 f^2 L^2}{V_I} \frac{M}{N} \quad (11)$$

It is found experimentally (ref. 3) that, if the entrance aperture is small relative to the field radius r_0 , the ion transmission through the quadrupole field will be maximum and independent of a/q (and hence independent of resolution) over most of the stability region, but will fall off rapidly near the peak of the stability region (fig. 4(d)).

The spectrometer is shown in figure 5. The approximation to a hyperbolic field by means of cylindrical rod electrodes was used where the radius of the stainless-steel rods is given by

$$r \simeq 1.16 r_0 \quad (12)$$

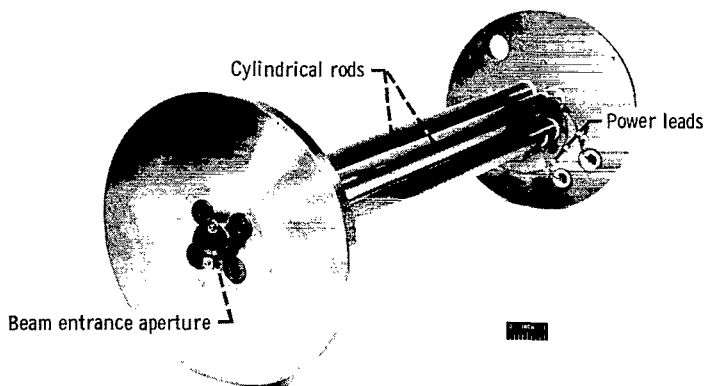


Figure 5. - Front view of analyzer section of electric quadrupole mass spectrometer. C-69557

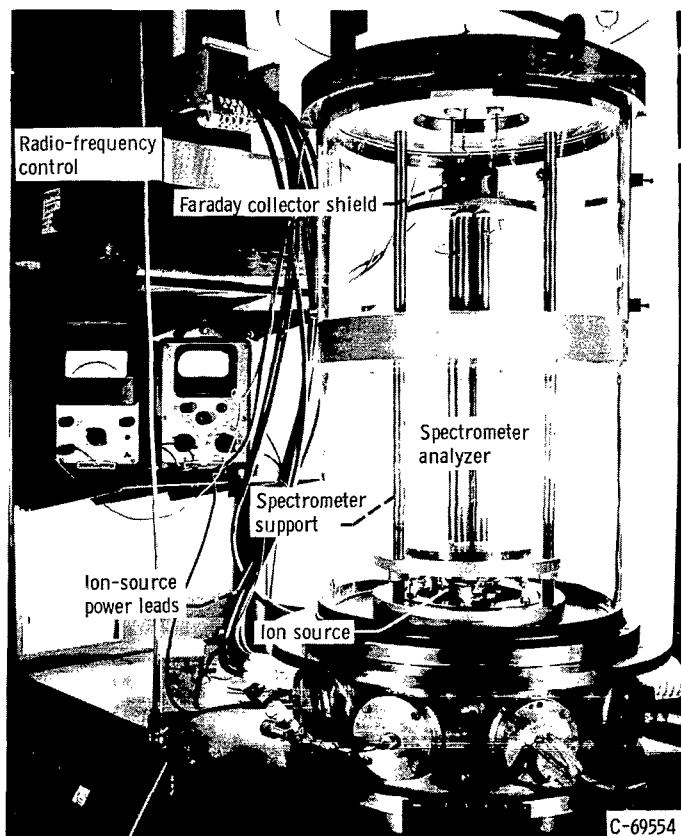


Figure 6. - Spectrometer and ion source in vacuum facility.

The value of r_0 used was 0.01 meter. The length of the rods was 0.50 meter. The rods were mounted to two stainless-steel plates and were electrically insulated from these plates with insulator rings. The entrance aperture was 2 millimeters in diameter. A collimating assembly was used to minimize the number of ions entering the spectrometer with transverse velocity components. This was done so as to minimize anomolous effects due to field fringing (ref. 6). A Faraday collector used to monitor the transmitted ion current was mounted through a ceramic insulator in a stainless-steel shield at the exit of the spectrometer.

Experimental configuration.

Figure 6 shows the experimental arrangement of the ion source and spectrometer in the vacuum facility. The ion source was mounted to a 1/16-inch steel O-ring by means of ceramic insulators. This assembly rested on a 1-inch-thick stainless-steel flange such that the source was seated in a 6-inch-diameter hole centered in the flange. All power leads and steam fittings were connected through port plates on the spool piece shown in figure 6. A copper plate with a 1-inch centered hole was mounted in front of the entrance aperture to the ion-source support and served to define the beam profile incident on the spectrometer.

The spectrometer rested on a

specially designed support that allowed for vertical alinement by means of adjusting three hex nuts supporting the base plate with the aid of an optical cathetometer. Electrical connections to the spectrometer were made through a 1-inch steel flange at the top of the 17-inch-inside diameter double-ended bell jar. A 6-inch oil diffusion pump served to maintain operating pressures ranging from 10^{-5} to 10^{-4} millimeter of mercury.

Procedure

Operation of ion source. - Some of the scaling properties of the ion source used in this investigation are described in reference 10. The anode voltage V_I (or net ion accelerating voltage) was maintained at 300 volts in order to (1) optimize the spectrometer resolving power and (2) prevent the occurrence of transient arcing between the source and external ground (the spectrometer and its support). The fact that electron emission currents J_E were less than 1 ampere resulted in very small ion beam currents (less than 1 ma). The mode of operation of the source was thus far from maximum efficiency conditions. In order to estimate the degree to which ionization in the discharge approximated that of a thruster, a comparison was made between mercury spectra obtained with this source and that reported in reference 15. The data employed in this comparison were obtained at a discharge voltage ΔV_I of 60 volts and net ion accelerating voltages of 500 and 1000 volts.

For operation with anthracene, the filament was first raised to emission temperatures (all other ion-source power supplied remaining off) in order to raise the temperature of the source and facilitate bakeout. The presence of foreign contaminants that could affect spectral measurements was minimized by allowing the system to outgas for

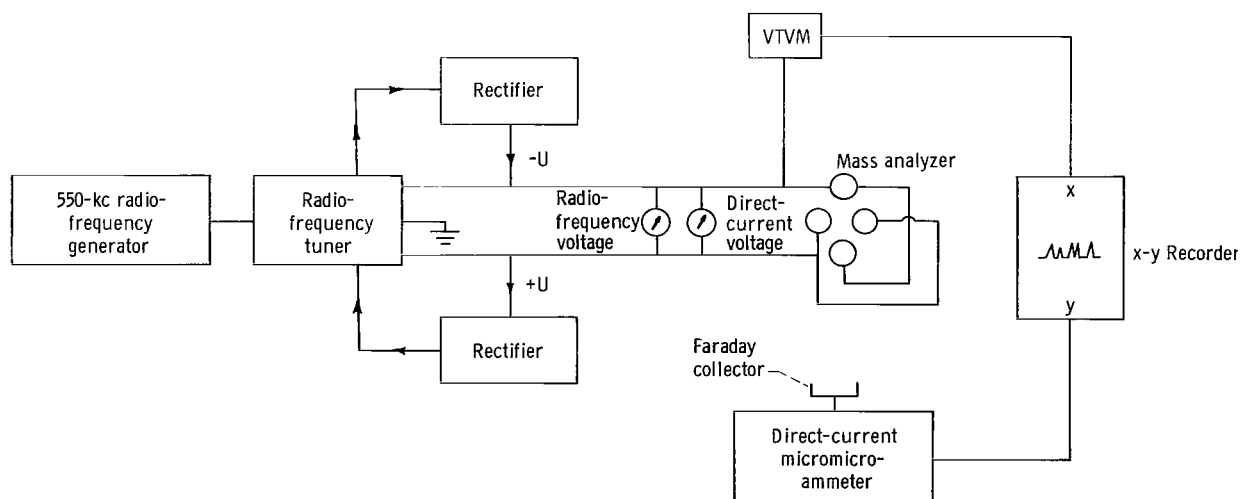


Figure 7. - Block diagram of spectrometer power supplies and detector equipment.

several hours prior to obtaining spectral traces.

Operation of the spectrometer. - In figure 7 a block diagram of the spectrometer, power supplies, and detector equipment is presented. The applied frequency was fixed at 550 kilocycles per second. The radio-frequency voltage could be varied over a range of 2400 volts (peak-to-peak) by means of a radio-frequency level control. The direct-current voltage was obtained by rectification of a portion of the radio-frequency voltage in such a manner that the ratio of the direct-current voltage to the radio-frequency voltage was constant over the sweep range. At the voltage ratios used ($2U/V = 0.30$ to 0.32), the transmission of all ion species was maximum.

The spectrometer was calibrated using known mass peaks of argon (A^+ , A^{++}) and mercury (Hg^+ , Hg^{++}). The resulting voltage calibration was such that the measured ratio $2U/V$ was accurate to within ± 3 percent.

Ion currents reaching the Faraday collector were monitored with a micromicroammeter. Ion current levels ranged from 10^{-11} to about 10^{-8} ampere.

Permanent spectral traces were obtained by connecting the x-axis of an X-Y recorder to the output amplifier of a vacuum tube voltmeter whose input was a portion of the applied radio-frequency voltage (fig. 7). The y-axis of the recorder was connected to the amplifier of the micromicroammeter used to monitor the Faraday collector current. The peak heights could thus be obtained directly.

The specific mass (M/N) values at the peaks were identified from equation (4) by using the measured radio-frequency voltage and the value $q = 0.706$ corresponding to the peak. The calculated specific masses coincided with specific masses reported in reference 9 to within ± 5 percent.

The maximum resolution attainable with the spectrometer used in this study was

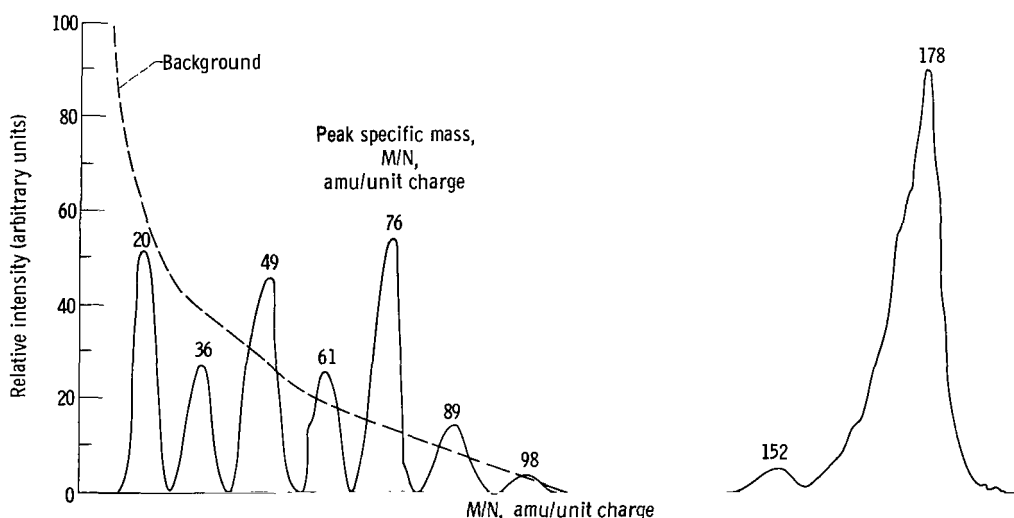


Figure 8. - Typical anthracene fragmentation spectra I. Operating conditions: discharge voltage, 40 volts; emission current, 10 milliamperes; net ion accelerating voltage, 300 volts.

$m/\Delta m = 40$. A search for peaks was undertaken at a $2U/V$ ratio corresponding to this resolution in order to locate all ion fragments. Measurements of spectral intensities were made from recorder traces obtained at values of $2U/V$ corresponding to maximum transmission. For these traces the resolution varied from about 5 at the low mass end of the spectrum to about 25 at the high mass end. The low and high specific mass limits with the present spectrometer were 20 and 900 atomic mass units per unit charge, respectively.

EXPERIMENTAL RESULTS AND DISCUSSION

Typical fragmentation spectra are presented in figures 8 and 9. The observed spectra contained seven to nine peaks representing specific masses ranging from 20 to 178 atomic mass units per unit charge. Their identification compared favorably with the molecular ions reported in reference 9 with the exception of masses 20 and 36, which were not reported in the reference.

The observed spectra were actually superimposed on a background current, as shown by the broken lines in figures 8 and 9, which was subtracted from the trace pattern in the actual presentation of peak heights. This background, which dropped to zero with increasing spectrometer voltages U and V , could be attributed to two effects. First, the selectivity of the spectrometer is greatly reduced at the low mass end of the spectrum, where spectrometer voltages are of the order of the net ion accelerating voltage. Hence, ions that should be deflected reach the collector. As the spectrometer voltage increases towards the high mass end of the spectrum, spectrometer selectivity increases and the

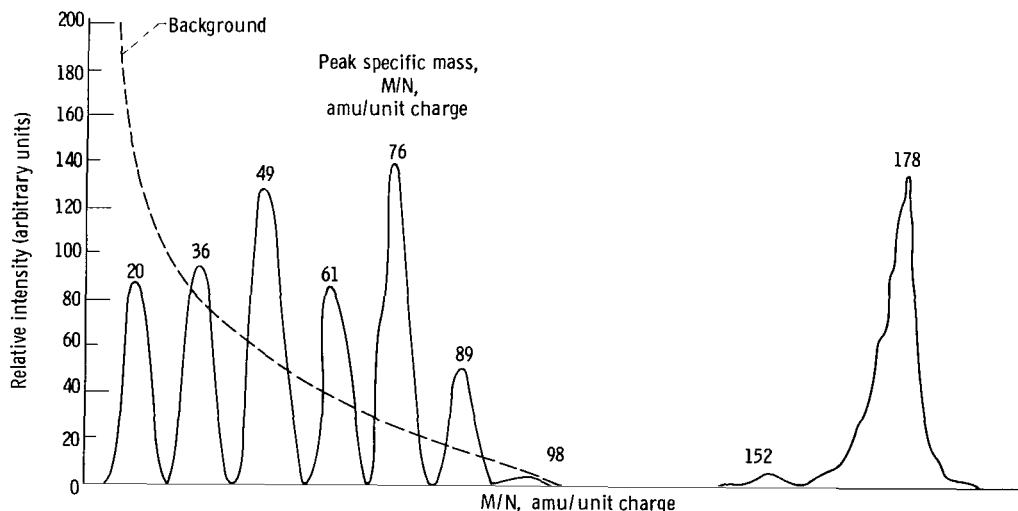


Figure 9. - Typical anthracene fragmentation spectra II. Operating conditions: discharge voltage, 80 volts; emission current, 10 milliamperes; net ion accelerating voltage, 300 volts.

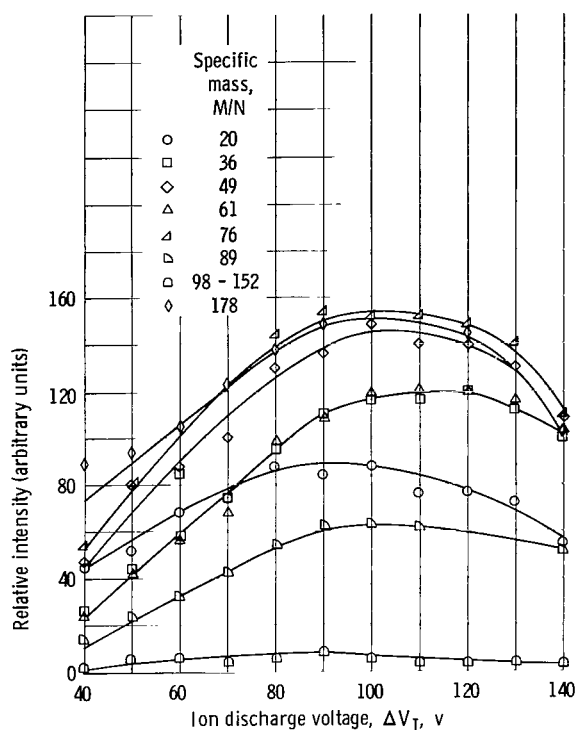


Figure 10. - Fragmentation of anthracene as function of ion discharge voltage. Electron emission, 10 milliamperes; net ion accelerating voltage, 300 volts.

tial. This was not the case in the present study. The difference between the usual yield curves and those of figure 10 is due to the nature of the discharge mechanism in the electron-bombardment ion source. Here the ignition of the discharge is determined by a balance between ion production and loss mechanisms in the plasma of the discharge chamber. The mean energy of the collision electrons required for a sustained discharge may be several electron volts greater than the ionization or dissociation energy of the molecule. For this reason the maxima of figure 10 occur at discharge voltages somewhat larger than might be expected from electron impact ion yield curves. The location of these maxima were found to vary only slightly with electron emission current.

The relative abundance of the different fragments, however, was highly dependent on the emission current, as is shown in figure 11. In general, the fragmentation was found to increase with the emission current, the relative proportion of low specific mass fragments rising with the discharge current. The plasma density of the discharge from which the data of figure 11 were obtained was in general greater than the density associated with the data of figure 10. This may account for the fact that specific masses 98 and 152 atomic mass units per unit charge appearing in figure 10 are absent from figure 11. The dependence of the ion yield on emission current can be understood on the basis of simple collision theory, which states that the number of ion species produced per unit volume

background current drops. The second contribution to background current may result from specific masses less than 20 atomic mass units per unit charge, which have sufficient velocity to traverse the quadrupole field undeflected.

Absolute peak currents were found to vary slightly from one trace to another although the ion-source operating point was unchanged. The relative peak heights did not change at a fixed operating point; thus only the relative peak heights can be considered significant in data interpretation.

Variation of the relative peak heights with ion discharge voltage (approximately mean electron energy) is presented in figure 10. These curves have the familiar form of ion yield curves in that maxima occur at particular electron energies (ref. 16). Normally, ion yield curves tend to peak at an electron energy corresponding to the ionization poten-

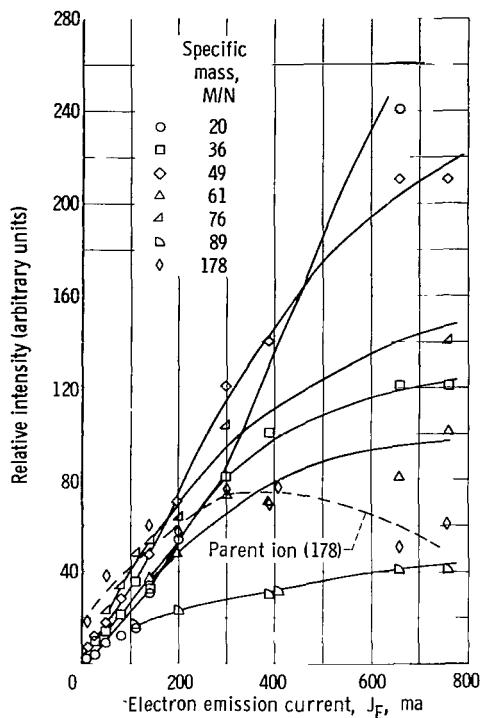


Figure 11. - Fragmentation of anthracene as function of electron emission. Discharge voltage, 50 volts; net ion accelerating voltage, 300 volts.

per unit time is dependent on the electron flux by the relation

$$\frac{dn_i}{dt} = n_o n_e v_e \sigma_i \quad (13)$$

where n_i is the number of ions produced per unit volume per unit time, n_o is the molecule density, n_e is the electron density, v_e is the electron speed, and σ_i is the ionization cross section. Multiplication by the electronic charge converts equation (13) into a current density relation, with $n_e e v_e$ representing the electron current density. Thus, at least to a first approximation, a linear dependence of ion yield on the emission current density is expected, the slope of the line being determined by the ionization cross section.

Within the limits of the sensitivity of the spectrometer no additional mass peaks were observed. If other species were present in significant amounts, they would have appeared as changes in line shapes and positions as source parameters were varied. No such changes were observed.

CONCLUDING REMARKS

Severe fragmentation of anthracene occurs in an electron-bombardment ion source operating with emission currents ranging from 10 to 760 milliamperes and discharge voltages ranging from 40 to 140 volts. This fragmentation is due primarily to the energetic electrons required to provide a sustained ion discharge. Severe fragmentation was observed even at the minimum conditions required to maintain the discharge. This result is in agreement with the conclusion of Byers, et al.; that is, fragmentation appears to be an inherent problem of electron-bombardment thrusters operating with a molecular propellant.

A comparison between mercury spectra obtained in the present source with that reported in the literature for a thruster indicated fair agreement in the measured ratio of doubly to singly ionized mercury. On the basis of this comparison, the ionization obtained in this study was estimated to approximate that of the thruster to within 15 percent.

Within the resolution capabilities of the spectrometer used in this investigation, a

maximum of nine ionized fragments in the range of 20 to 178 atomic mass units per unit charge were observed at the discharge conditions employed.

Lewis Research Center,
National Aeronautics and Space Administration,
Cleveland, Ohio, October 30, 1964.

APPENDIX - SYMBOLS

a	parameter defined in eq. (3), dimensionless	U	applied direct-current voltage, v
e	electronic charge, 1.6×10^{-19} coulomb	V	applied radio-frequency voltage amplitude, v
f	frequency of applied radio-frequency field, Mcps	$V/\Delta V$	resolution, dimensionless
J_E	electron emission cur- rent, ma	V_A	accelerator voltage, v
L	length of quadrupole spectrometer, m	V_I	net ion accelerating voltage, v
M	ion mass, amu	ΔV_I	ion discharge voltage, v
m	ion mass at peak maximum, kg	v_e	electron velocity, cm/sec
$m/\Delta m$	resolution, dimensionless	x, y	transverse displacement of ion trajectory, cm
N	number of electronic charge per ion	x'', y'', z''	second-order differentia- tion with respect to ξ , cm/sec ²
n_i	number of ions produced per unit volume	z	axial displacement of ion trajectory, cm
dn_i/dt	time derivative of ion density, cm ⁻³ sec ⁻¹	ξ	dimensionless time varia- ble, $\omega t/2$
n_o	molecule density, cm ⁻³	τ_i	ionization cross section, cm ²
n_e	electron density, cm ⁻³	Φ	potential of focusing field (eq. (2)), v
q	parameter defined in eq. (4), dimensionless	Φ_o	form of applied voltages (eq. (1)), v
r	radius of spectrometer rods, m	ω	angular frequency of applied electric field, sec ⁻¹
r_o	radius of spectrometer focusing field, m		
t	time, sec		

REFERENCES

1. Mickelsen, William R.: NASA Research on Heavy-Particle Electrostatic Thrustors. Paper 63-19, IAS, 1963.
2. Byers, David C., Kerslake, William R., and Grobman, Jack: Experimental Investigation of Heavy-Molecule Propellants in an Electron-Bombardment Thrustor. NASA TN D-2401, 1964.
3. Paul, W., Reinhard, H. P., and von Zahn, U.: The Electric Mass Filter as a Mass Spectrometer and Isotope Separator. TR-3484, AEC, 1958. (Trans. from Zs. Physik, vol. 152, 1958, pp. 143-182.)
4. Mosharrafa, M., and Oskan, H. J.: Design and Construction of a Mass-Spectrometer for the Study of Basic Processes in Plasma Physics. Tech. Rep. 2, July 1960-July 1961.
5. Woodward, C. E., and Crawford, C. K.: Design of a Quadrupole Mass Spectrometer. TR 176, M.I.T., Jan. 1963.
6. Brubaker, Wilson M.: The Quadrupole Mass Filter. Instruments and Measurements, Academic Press, 1961, pp. 325-331.
7. Hertzberg, M.: A Strong Focusing Mass Spectrometer. Proc. Atomic and Molecular Beams Conf., Univ. Denver, Denver (Colo.), June 20-22, 1960, pp. 79-94.
8. Dugan, John V., Jr.: Some Theoretical Bases for Selection of Molecular Ion Propellants and a Survey of Molecular Plasma Collision Processes. NASA TN D-1185, 1964.
9. Wacks, Morton E., and Dibeler, Vernon H.: Electron Impact Studies of Aromatic Hydrocarbons. I. Benzene, Napthalene, Anthracene, and Phenanthrene. Jour. Chem. Phys., vol. 31, no. 6, Dec. 1959, pp. 1557-1562.
10. Reader, P. D.: Scale Effects on Ion Rocket Performance. ARS Jour., vol. 32, no. 5, May 1962, pp. 711-714.
11. Kaufman, Harold R.: An Ion Rocket with an Electron-Bombardment Ion Source. NASA TN D-585, 1961.
12. Kaufman, Harold R., and Reader, Paul D.: Experimental Performance of Ion Rockets Employing Electron-Bombardment Ion Sources. Paper 1374-60, ARS, 1960.
13. Reader, Paul D.: Investigation of a 10-Centimeter-Diameter Electron-Bombardment Ion Rocket. NASA TN D-1163, 1962.

14. McLachlan, N. W.: Theory and Application of Mathieu Functions. Oxford Univ. Press, 1947.
15. Milder, Nelson L.: Comparative Measurements of Singly and Doubly Ionized Mercury Produced by Electron-Bombardment Ion Engine. NASA TN D-1219, 1962.
16. Massey, H. S. W., and Burhop, E. H. S.: Electronic and Ionic Impact Phenomena. Oxford Univ. Press, 1952.

2 11/85
92

"The aeronautical and space activities of the United States shall be conducted so as to contribute . . . to the expansion of human knowledge of phenomena in the atmosphere and space. The Administration shall provide for the widest practicable and appropriate dissemination of information concerning its activities and the results thereof."

—NATIONAL AERONAUTICS AND SPACE ACT OF 1958

NASA SCIENTIFIC AND TECHNICAL PUBLICATIONS

TECHNICAL REPORTS: Scientific and technical information considered important, complete, and a lasting contribution to existing knowledge.

TECHNICAL NOTES: Information less broad in scope but nevertheless of importance as a contribution to existing knowledge.

TECHNICAL MEMORANDUMS: Information receiving limited distribution because of preliminary data, security classification, or other reasons.

CONTRACTOR REPORTS: Technical information generated in connection with a NASA contract or grant and released under NASA auspices.

TECHNICAL TRANSLATIONS: Information published in a foreign language considered to merit NASA distribution in English.

TECHNICAL REPRINTS: Information derived from NASA activities and initially published in the form of journal articles.

SPECIAL PUBLICATIONS: Information derived from or of value to NASA activities but not necessarily reporting the results of individual NASA-programmed scientific efforts. Publications include conference proceedings, monographs, data compilations, handbooks, sourcebooks, and special bibliographies.

Details on the availability of these publications may be obtained from:

SCIENTIFIC AND TECHNICAL INFORMATION DIVISION
NATIONAL AERONAUTICS AND SPACE ADMINISTRATION

Washington, D.C. 20546